

# Flavor dependence of the nucleon valence structure from nuclear deep inelastic scattering data

E.P. Segarra,<sup>1</sup> A. Schmidt,<sup>1</sup> D.W. Higinbotham,<sup>2</sup> T. Kutz,<sup>3</sup>  
 E. Piasetzky,<sup>4</sup> M. Strikman,<sup>5</sup> L.B. Weinstein,<sup>6</sup> and O. Hen<sup>1,\*</sup>

<sup>1</sup>*Massachusetts Institute of Technology, Cambridge, Massachusetts 02139, USA*

<sup>2</sup>*Thomas Jefferson National Accelerator Facility, Newport News, Virginia 23606*

<sup>3</sup>*Stony Brook University, Stony Brook, NY 11794, USA*

<sup>4</sup>*School of Physics and Astronomy, Tel Aviv University, Tel Aviv 69978, Israel*

<sup>5</sup>*Pennsylvania State University, University Park, PA, 16802*

<sup>6</sup>*Old Dominion University, Norfolk, Virginia 23529*

(Dated: May 10, 2022)

The partonic structure of the nucleon in the valence region is studied using a global analysis of nuclear deep inelastic scattering (DIS) data on the proton and on nuclei from  $A = 2$  (deuterium) to 208 (lead) to account for the modification of the structure function of nucleons bound in atomic nuclei (i.e. the EMC effect). As compared to previous analyses that only use proton and deuterium data, we find a larger valence down-quark contribution at high- $x_B$ . The neutron-to-proton structure function ratio  $F_2^n/F_2^p$  is extracted for  $x_B = 0.2-0.9$ , with an  $x_B \rightarrow 1$  limit of  $0.47 \pm 0.04$ , in agreement with predictions such as those of perturbative QCD and Dyson-Schwinger equation expectations, but in disagreement with predictions such as the scalar di-quark dominance model. Predictions are also made for  $F_2^{^3\text{He}}/F_2^{\text{H}}$ , recently measured by the MARATHON collaboration, the nuclear correction function that is needed to extract  $F_2^n/F_2^p$  from  $F_2^{^3\text{He}}/F_2^{\text{H}}$ , and the systematic uncertainty associated with this extraction.

## INTRODUCTION

Since the discovery of quarks and gluons (partons) and the subsequent development of QCD, significant experimental and theoretical effort has gone into determining the distributions of partons in hadrons. Measurements of lepton Deep Inelastic Scattering (DIS) from protons and neutrons should allow for extraction of the distributions of both up ( $u$ ) and down ( $d$ ) quarks in the nucleon. The lack of a free neutron target prevents such a direct extraction. Therefore, global analyses commonly use deuterium as a proton+neutron target. This results in incomplete knowledge of the  $d$ -quark distribution due to incomplete knowledge of the required nuclear corrections to the deuterium data.

While exact SU(6) symmetry implies that the valence  $d$ - to  $u$ -quark ratio in the proton,  $d_v/u_v$ , should equal 1/2, the mass difference between the nucleon and the Delta resonance indicates that SU(6) symmetry is broken. The exact symmetry-breaking mechanism is still unknown. Different symmetry breaking models predict different limits of  $d_v(x_B)/u_v(x_B)$  as  $x_B \rightarrow 1$  (where  $x_B = Q^2/2mv$ ,  $Q^2$  is the four-momentum transfer squared,  $m$  is the nucleon mass and  $\nu$  is the energy transfer), see e.g. [1–5].

The limit of  $x_B = 1$  corresponds to elastic scattering. Knowledge of  $d_v/u_v$  in this limit can therefore provide information about the flavor dependence of the proton form factors at  $Q^2 = 0$  [4, 6]. In addition, under DGLAP evolution, parton distributions at low- $Q^2$  and high- $x_B$  determine their behavior at high- $Q^2$  and low- $x_B$ , which are important for high-energy collider experiments.

In the simple parton model,  $d_v/u_v$  can be inferred from the neutron-to-proton structure function ratio  $F_2^n(x_B)/F_2^p(x_B)$  by assuming isospin symmetry and cancellation of dynamic higher-twist effects [7] such that

$$\frac{d_v}{u_v} = \frac{4F_2^n/F_2^p - 1}{4 - F_2^n/F_2^p}, \quad (1)$$

with  $F_2^n$  being traditionally extracted from analyses of proton and deuterium data. The structure functions are functions of both  $x_B$  and  $Q^2$ . For brevity we omit this dependence and write  $F_2$  and  $d_v$  rather than  $F_2(x_B, Q^2)$  and  $d_v(x_B)$ .

Such extraction of  $F_2^n$  from  $F_2^p$  and  $F_2^d$  requires accurate accounting for nuclear effects in the deuteron that include the binding energy and motion of the nucleons, as well as the difference between the structure functions of nucleons bound in nuclei and those of free nucleons. Calculations of the effects of binding energy and nucleon motion are well established, and their impact is generally understood (see e.g. Refs. [8–13] and the references therein). However, bound nucleon structure is not well understood.

The most direct experimental evidence for the difference between bound and free nucleon structure functions in the valence region comes from the observation of the EMC effect, a deviation from unity of the measured per-nucleon deep inelastic scattering (DIS) cross-section ratio for nuclei relative to deuterium, see Ref. [14, 15] for a recent review. An EMC-like effect in the deuteron would make  $F_2^d \neq F_2^p + F_2^n$ , even after accounting for binding and nucleon motion. This difference needs to be taken into account in extracting  $F_2^n$ . Different analyses

address these effects in different ways, from analyzing only selected data measured in kinematics where they are thought to be suppressed, to using large data samples with different theoretical models for the corrections [12, 13, 16–18].

Here we perform a global analysis of DIS data in nuclei from  $A = 1$  (proton) to 208 (Pb) to consistently account for the EMC effect and determine the difference between the free and bound nucleon structure functions [19]. We use that difference to extract  $F_2^n/F_2^p$  from  $F_2^p$  and  $F_2^d$ . We also use our analysis to predict the EMC effect in tritium, and to estimate the nuclear correction function that is needed to extract  $F_2^n/F_2^p$  from the measurements of  $F_2^{^3\text{He}}/F_2^{^3\text{H}}$ . By comparing our new nuclear correction function with those of earlier works we quantify the model uncertainty associated with such extractions of  $F_2^n/F_2^p$ .

## UNIVERSAL NUCLEON MODIFICATION AND THE EMC EFFECT

This paper accounts for the EMC effect in nuclear DIS data by exploiting the insight to the origin of the EMC effect recently obtained from observations of a correlation between the magnitude of the EMC effect in different nuclei and the relative amount of short-range correlated (SRC) nucleon pairs in those nuclei [8, 15, 19–22].

SRCs are predominantly proton-neutron ( $pn$ ) pairs [23–28]. They have large relative and individual momenta, small center-of-mass momenta, and account for 60–70% of the kinetic energy carried by nucleons in the nucleus [25, 29–31]. Therefore, nucleons in such pairs have significant spatial overlap and are far off their mass-shell ( $E^2 - p^2 - m^2 < 0$ ). These extreme conditions and the observed correlation between SRC abundances and the magnitude of the EMC effect imply that the EMC effect could be driven primarily by the modification of the structure function of nucleons in SRC pairs rather than those of all nucleons [15, 20, 21].

Utilizing scale separation between SRC and uncorrelated (mean-field) nucleons, Ref. [19] modeled the nuclear structure function as having contributions from unmodified uncorrelated nucleons and from modified correlated nucleons in  $np$ -SRC pairs:

$$F_2^A = ZF_2^p + NF_2^n + n_{SRC}^A(\Delta F_2^p + \Delta F_2^n), \quad (2)$$

where  $N$  and  $Z$  are the number of neutrons and protons in the nucleus ( $N + Z = A$ ),  $n_{SRC}^A$  is the average number of nucleons in SRC pairs, and  $\Delta F_2^p$  and  $\Delta F_2^n$  are the average difference between the structure function of free nucleons and nucleons in SRC pairs. This model assumes that both the EMC effect at  $0.3 \leq x_B \leq 0.7$  and the nucleon-motion effects that dominate at  $x_B > 0.7$  are dominated by SRCs. Therefore both these effects are

approximately proportional to the SRC abundances [9, 32] and both captured in our flexible parameterization of the structure modification. This model neglects the  $\approx 10\%$  of  $NN$  SRC pairs that are  $pp$  or  $nn$ .

To reduce sensitivity to isospin and higher twist effects [7], DIS data are traditionally given in the form of  $F_2^A/F_2^d$ . We therefore use Eq. 2 to express this ratio as:

$$\begin{aligned} \frac{F_2^A}{F_2^d} &= \frac{\Delta F_2^p + \Delta F_2^n}{F_2^d/n_{SRC}^d} \times \left( \frac{n_{SRC}^A}{n_{SRC}^d} - N \right) + (Z - N) \frac{F_2^p}{F_2^d} + N \\ &= f_{\text{univ}}(x_B) \times \left( \frac{n_{SRC}^A}{n_{SRC}^d} - N \right) + (Z - N) \frac{F_2^p}{F_2^d} + N, \end{aligned} \quad (3)$$

where we defined a universal modification function (UMF)

$$f_{\text{univ}} = n_{SRC}^d \frac{\Delta F_2^p + \Delta F_2^n}{F_2^d}$$

that should be nucleus independent. Consistent UMFs were previously extracted for nuclei from  $^3\text{He}$  to  $^{208}\text{Pb}$ , pointing to the existence of a global UMF for SRC pairs in any nucleus (see Fig. 1) [19]. Here we extract the global UMF using Bayesian inference by means of a Hamiltonian Markov Chain Monte Carlo (HMCMD) [33, 34], referred to herein as Nuclear-DIS analysis.

We parametrized the UMF for all nuclei as

$$f_{\text{univ}} = \alpha + \beta x_B + \gamma e^{\delta(1-x_B)}$$

and estimated its parameters ( $\alpha$ ,  $\beta$ ,  $\gamma$ , and  $\delta$ ) using HMCMD-based inference from world  $F_2^A/F_2^d$  data [19, 35, 36] for  $0.08 \leq x_B \leq 0.95$  from  $^3\text{He}$ ,  $^4\text{He}$ ,  $^9\text{Be}$ ,  $^{12}\text{C}$ ,  $^{27}\text{Al}$ ,  $^{56}\text{Fe}$ ,  $^{197}\text{Au}$ , and  $^{208}\text{Pb}$ , via Eq. 3. We assumed  $\frac{n_{SRC}^A}{n_{SRC}^d/2} = a_2(A/d)$ , the average per-nucleon cross-section ratio for quasi-elastic electron scattering in nucleus  $A$  relative to deuterium at  $1.5 < x_B < 2$  [19, 37].  $F_2^p/F_2^d$  is taken from Table 2 of Ref. [38]. As consistent parameterizations of  $F_2^p/F_2^d$  as a function of  $x_B$  are needed for the UMF extraction, we parametrized it as  $F_2^p/F_2^d = \alpha_d + \beta_d x_B + \gamma_d e^{\delta_d(1-x_B)}$  and determined its parameters simultaneously as part of the Nuclear-DIS analysis.

We assumed that the experimental point-to-point uncertainties on individual  $F_2^A/F_2^d$  data points and the overall normalization uncertainties each represented the standard deviation of a normal distribution. We did not apply isoscalar corrections to the data for neutron-rich nuclei. See online supplementary materials for details on the inference procedure and resulting posterior distribution for the parameters.

The different data-sets used in this analysis were obtained at different values of invariant hadronic mass,  $W$ , and  $Q^2$ . For  $W^2 > 2 \text{ GeV}^2$  and  $Q^2 > 2 \text{ GeV}^2$ , the ratio  $F_2^A/F_2^d$  was shown to be largely insensitive to higher twist effects, as evident by its  $Q^2$  independence [19, 35, 36, 39].

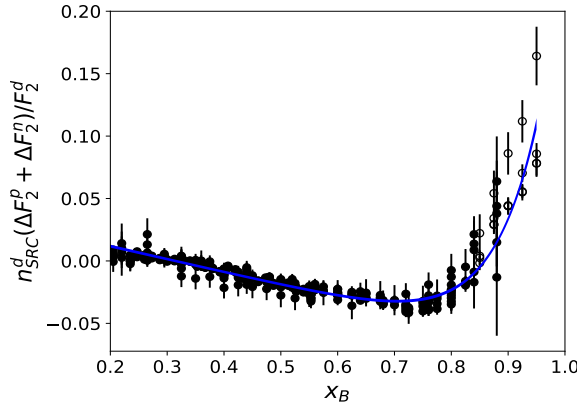


FIG. 1: The extracted universal modification function (UMF) from the Nuclear-EMC effect analysis performed here. The width of the band shows the 68% confidence interval. Data points show the data-driven extractions of Ref. [19], based on individual measurements of  $F_2^A/F_2^d$  in a variety of nuclei. Closed and open data points show measurements at  $W^2 > 2$   $\text{GeV}^2$  and  $W^2 < 2$   $\text{GeV}^2$  respectively.

At  $x_B \geq 0.8$ , where the data are predominantly at  $W^2 < 2$   $\text{GeV}^2$ , this  $Q^2$ -independence was demonstrated over a smaller range. We therefore assume that  $F_2^A/F_2^d$  is  $Q^2$ -independent, but indicate the region of  $x_B > 0.8$  which includes the low  $W^2$  data. Lastly, as  $F_2^p/F_2^d$  does show some  $Q^2$  dependence, we use  $F_2^p/F_2^d$  extracted at  $Q_0^2 = 12$   $\text{GeV}^2/c^2$  [38], which is consistent with the  $Q^2$  range of the  $F_2^A/F_2^d$  data sets.

The Nuclear-DIS analysis reproduced all the  $F_2^A/F_2^d$  data over the entire measured  $x_B$  range (see online supplementary materials). The resulting global UMF is shown as a band in Fig. 1, compared with the point-by-point extracted UMFs for individual nuclei. The global UMF has very small uncertainty and agrees well with the individual nuclear UMFs extracted in Ref [19]. The parameters' posterior distributions are mostly uncorrelated (see online supplementary materials for the full correlation matrix). The constant and linear parameters,  $\alpha$  and  $\beta$ , exhibit a small correlation (Pearson  $r = -0.752$ ) and the exponent coefficients,  $\gamma$  and  $\delta$ , exhibit an even smaller correlation ( $r = -0.717$ ).

The extracted UMF extends up to  $x_B \sim 0.95$ . As discussed below, for  $x_B > 0.8$  the available data is primarily at  $W^2 < 2$   $\text{GeV}^2$ , well below the deep inelastic region [39]. In addition, at  $x_B \geq 0.9$ , the experimental data is less accurate and likely more  $Q^2$ -dependent.

The posterior prefers that the measured  $^3\text{He}$  EMC ratio [36] be re-scaled by about 2%, which is at the higher end of its quoted normalization uncertainty and is consistent with the independent renormalization of Ref. [40].

As mentioned, we neglected the contribution of proton-proton ( $pp$ ) and neutron-neutron ( $nn$ ) SRC pairs. For symmetric nuclei, introducing  $pp$ - and  $nn$ -SRC pairs to Eqs. 2 and 3 will not affect the extracted UMF if nucleon

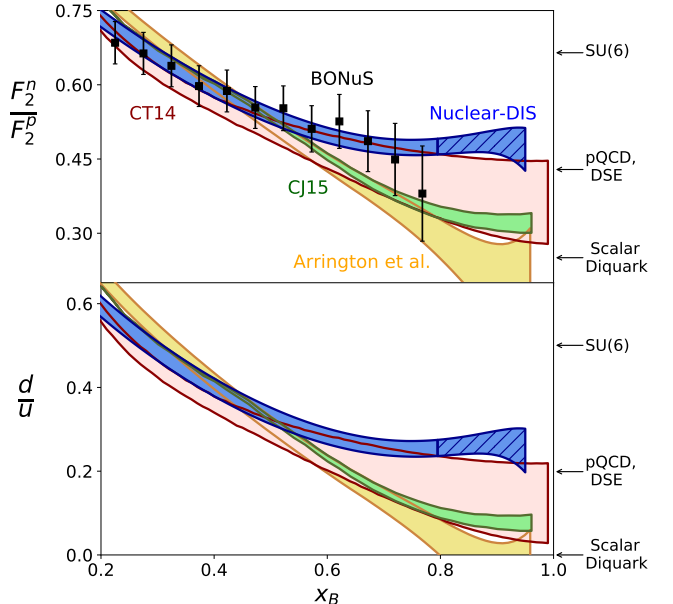


FIG. 2: Neutron-to-proton structure function ratio  $F_2^n/F_2^p$  (top) and down-to-up valence quark distribution ratio (bottom). Data points show the  $d(e, e' p_S)$  tagged-DIS measurement [41]. The blue band labeled ‘Nuclear-DIS’ shows the results of the Nuclear-DIS analysis done here. CJ15 [13] (green band) and CT14 [16] (red band) show the global analysis of proton and deuterium data with and without accounting for nuclear effects, respectively. Arrington, et al. [17] (yellow band), shows an extraction based on proton and deuterium data that accounts only for Fermi-motion and binding effects in the deuteron. The labels show the predictions at  $x_B = 1$  such as of the SU(6) symmetry [42], the perturbative QCD (pQCD) [1], the Dyson-Schwinger Equation (DSE) [6] and the Scalar Diquark models [43, 44]. All extractions were consistently evolved to the same value of  $Q^2$  based on the kinematics of the MARATHON experiment [45], i.e.  $Q^2 = (14 \text{ GeV}^2) \times x_B$ . See online supplementary materials for details.

modification is the same in  $nn$ ,  $pp$  and  $np$  pairs (see online supplementary materials). For asymmetric nuclei, including the effects of  $nn$  and  $pp$  pairs could change the UMF by a few percent.

### EXTRACTION OF $d_v/u_v$ AND $F_2^n/F_2^p$

The UMF accounts for nuclear effects in  $F_2^d$ , allowing us to express  $F_2^n/F_2^p$  as:

$$\frac{F_2^n}{F_2^p} = \frac{1 - f_{\text{univ}}}{F_2^p/F_2^d} - 1. \quad (4)$$

We use the continuous parameterizations of both  $f_{\text{univ}}$  and  $F_2^p/F_2^d$  from the Nuclear-DIS analysis of the previous section to extract  $F_2^n/F_2^p$  and to calculate  $d_v/u_v$  (see Fig. 2). Our results are consistent with the experimental

extraction using tagged  $d(e, e' p_S)$  DIS measurements on the deuteron Ref. [41].

Both  $F_2^n/F_2^p$  and  $d_v/u_v$  decrease steadily for  $x_B \geq 0.2$  and become approximately constant at  $x_B \approx 0.65$ . The limit of  $F_2^n/F_2^p$  as  $x_B \rightarrow 1$  is about 0.47 which corresponds to  $d_v/u_v = 0.23$ . This value agrees with theoretical predictions such as those based on perturbative QCD [1] and the Dyson-Schwinger Equation (DSE) [6] and is inconsistent predictions such as the Scalar Diquark model prediction [43, 44]. Thus, accounting for the modification of nucleons bound in deuterium increases the  $d$ -quark contribution to the proton at high- $x_B$ . While in this work  $d_v/u_v$  is calculated following Eqn. 1, see online supplementary materials for a discussion on target-mass and next-to-leading order corrections.

Removing the  $W^2 < 2 \text{ GeV}^2$  data from the Nuclear-DIS analysis limits our extraction to  $x_B \sim 0.8$ . However, it does not change the functional form of the extraction for  $x_B < 0.8$ . As  $F_2^n/F_2^p$  becomes constant  $x_B \approx 0.65$ , removing the low  $W$  data does not change our conclusions. Similarly, we verified that evolving  $F_2^n/F_2^p$  extracted at  $Q_0^2 = 12 \text{ GeV}^2/c^2$  down to  $Q^2 = 5 \text{ GeV}^2/c^2$  does not impact our extraction of  $F_2^n/F_2^p$  up to  $x_B \sim 0.8$ . See online supplementary materials for details.

Our Nuclear-DIS analysis gives larger values of  $F_2^n/F_2^p$  and  $d_v/u_v$  than previous extractions. Fig. 2 shows our results compared with three previous extractions that used only proton and deuterium data: (A) CTEQ global analysis (CT14) which uses high- $W$  data ( $> 3.5 \text{ GeV}$ ) with no corrections for any nuclear effects in the deuteron, (B) CTEQ-JLab global analysis (CJ15) which uses lower- $W$  data ( $> 1.73 \text{ GeV}$ ) and includes corrections for both Fermi motion and binding and for structure-modification of the bound nucleon structure within a nucleon swelling model, and (C) Arrington et al., which includes only corrections for Fermi motion and binding but not for structure-modification of the bound nucleon. The comparison with CJ15 is particularly interesting as that extraction of  $d(x_B)/u(x_B)$  is predominately constrained by the D $\emptyset$   $W^\pm$  boson asymmetry data [13, 46], corresponding to  $Q^2 = m_W^2$ . This may indicate a tension between our low  $Q^2$  results and results of the CJ15 analysis of the D $\emptyset$  dataset at  $x_B \geq 0.6$ . We emphasize that the CJ15  $F_2^n/F_2^p$  band was calculated using their extracted  $d/u$  with Eqn. 1.

Our analysis also differs in its treatment of medium modification effects in the deuteron which is largely driven by the heavy nuclei data. As deuteron is a special case (only few percent SRC, very small binding energy, etc.) we performed a separate analysis where we scaled the deuteron modification by a factor  $\lambda \in [0, 1]$ , which was added to the model as an additional parameter. This exercise resulted in identical extraction up to  $x_B \sim 0.8$  and only a very small variation above it. See online supplemental materials for details.

Previous studies have shown that accounting for

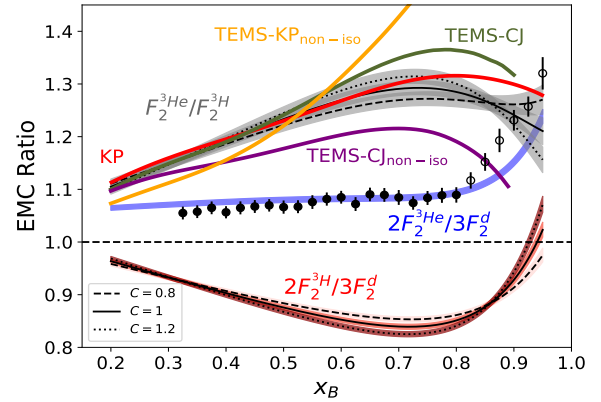


FIG. 3: Nuclear-DIS analysis results for  $2F_2^{^3\text{He}}/3F_2^d$ ,  $2F_2^{^3\text{H}}/3F_2^d$  and  $F_2^{^3\text{He}}/F_2^{^3\text{H}}$  (full bands). The width of the bands show the 68% confidence intervals of our analysis. The three black line types show the Nuclear-DIS analysis predictions for different assumptions on  $n_{^3\text{SRC}}^{^3\text{He}}/n_{^3\text{SRC}}^d = C \times n_{^3\text{SRC}}^{^3\text{He}}/n_{^3\text{SRC}}^d$ . Symbols show the  $2F_2^{^3\text{He}}/3F_2^d$  measurement of Ref. [36] and labeled lines show previous extractions of  $F_2^{^3\text{He}}/F_2^{^3\text{H}}$  by Tropiano et al. [18] (TEMs [green, purple, orange, assuming different off-shell corrections]) and Kulagin and Pettit [40, 50] (KP [red]). See text for details.

structure-modification of the bound nucleon structure increases  $F_2^n/F_2^p$  at high- $x_B$ , see e.g. Ref. [3, 8, 47–49]. However, the magnitude of this increase is smaller for the analyses that only use deuterium data as compared with our nuclear-DIS analysis that consistently accounts for nuclear target data from deuterium to lead.

#### $d_v/u_v$ : EXTRACTION FROM $A = 3$ MIRROR-NUCLEI DATA

Another independent extraction of  $F_2^n/F_2^p$  will be done by the MARATHON experiment that recently measured DIS off  $d$ ,  ${}^3\text{He}$  and  ${}^3\text{H}$  [45]. They plan to extract  $F_2^n/F_2^p$  from the measured  $F_2^{^3\text{He}}/F_2^{^3\text{H}}$  ratio using [45]:

$$\frac{F_2^n}{F_2^p} = \frac{2\mathcal{R} - F_2^{^3\text{He}}/F_2^{^3\text{H}}}{2F_2^{^3\text{He}}/F_2^{^3\text{H}} - \mathcal{R}}, \quad (5)$$

where  $\mathcal{R}$  is a measure of the cancellation of nuclear effects in the  $F_2^{^3\text{He}}/F_2^{^3\text{H}}$  ratio:

$$\mathcal{R} \equiv \frac{F_2^{^3\text{He}}}{2F_2^p + F_2^n} \times \frac{F_2^p + 2F_2^n}{F_2^{^3\text{H}}}, \quad (6)$$

and is taken from theoretical calculations.

We used our universal function to predict the expected DIS ratios for  $[F_2^{^3\text{He}}/3]/[F_2^d/2]$ ,  $[F_2^{^3\text{H}}/3]/[F_2^d/2]$  and  $F_2^{^3\text{He}}/F_2^{^3\text{H}}$  (see Fig. 3). Since  $n_{^3\text{SRC}}^{^3\text{H}}/n_{^3\text{SRC}}^d$  is not yet published, we calculated the expected results for three possibilities,  $n_{^3\text{SRC}}^{^3\text{H}}/n_{^3\text{SRC}}^d = C \times n_{^3\text{SRC}}^{^3\text{He}}/n_{^3\text{SRC}}^d$  with

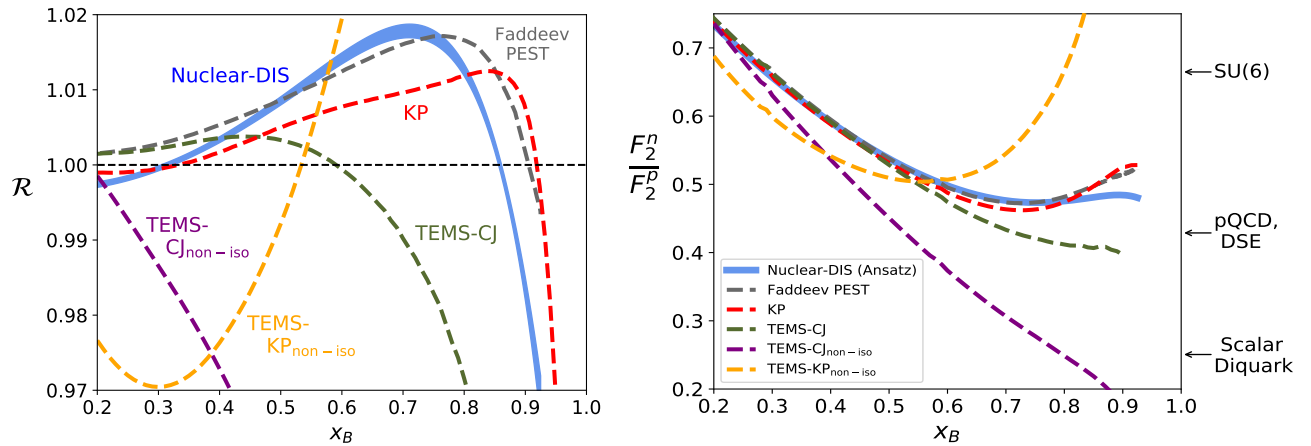


FIG. 4: Left: Different model predictions for  $\mathcal{R}$  as defined in Eq. 6. Blue band labeled ‘Nuclear-DIS’ shows the 68% confidence intervals of the Nuclear-DIS analysis done here. The other labeled lines show calculations by Tropiano et al. [18] (TEMS, for different off-shell corrections), Kulagin and Pett [40, 50] (KP), and Afan et al. [51] (PEST). Right:  $F_2^n/F_2^p$  extracted from  $F_2^{^3\text{He}}/F_2^{^3\text{H}}$  using different models for  $\mathcal{R}$  (see Eq. 5). All extractions used the same Nuclear-DIS model prediction for  $F_2^{^3\text{He}}/F_2^{^3\text{H}}$  (labeled ‘Ansatz’) with different models for  $\mathcal{R}$ . See text for details.

$C = 0.8, 1.0$  and  $1.2$ . The results show little sensitivity to the value of  $C$ .

We compare our predictions for the  $F_2^{^3\text{He}}/F_2^{^3\text{H}}$  ratio to those of other theoretical models, shown as colored lines in Fig. 3. Our prediction is similar to that of Kulagin and Pett [40, 50], and only slightly disagrees for  $x_B > 0.8$ . The Tropiano et al. [18] predictions (labeled TEMS) combine the CJ15 PDF global fits, CJ15 nuclear off-shell corrections applied to deuterium, and additional fits to  $^3\text{He}$  EMC ratio data [36], in order to extract off-shell corrections in  $A = 3$  nuclei. TEMS-CJ assumes fully isoscalar off-shell corrections, TEMS-CJ<sub>non-iso</sub> assumes non-isoscalar corrections, and TEMS-KP<sub>non-iso</sub> uses the non-isoscalar off-shell corrections developed by Kulagin and Pett [40]. Our model prediction falls within the band of possibilities predicted by TEMS-CJ and TEMS-KP. The spread of model predictions and sensitivity to non-isoscalar modification demonstrate the need for the MARATHON measurements.

We also predicted the nuclear effect ratio  $\mathcal{R}$  (see Fig. 4, left panel). To see the dependence of  $F_2^n/F_2^p$  on  $\mathcal{R}$ , we used the predicted  $F_2^{^3\text{He}}/F_2^{^3\text{H}}$  from our Nuclear-DIS analysis and extracted  $F_2^n/F_2^p$  using the different models of  $\mathcal{R}$  (see Fig. 4, right panel). The variation in the results indicates a model uncertainty at large- $x_B$ , in agreement with previous studies [52]. Different assumptions about the underlying behavior of  $F_2^{^3\text{He}}/F_2^{^3\text{H}}$  give similar variation, see supplementary materials.

This systematic model uncertainty will be fully quantified once measurements of  $F_2^{^3\text{He}}/F_2^{^3\text{H}}$  are available, by iterating the value of  $F_2^n$  extracted by Eq. 5 and used by Eq. 6. However, any iteration of  $F_2^n$  must be consistent with nuclear DIS data.

## CONCLUSIONS

We extracted a nucleon universal modification function that is consistent with measurements of the deep inelastic structure functions of nuclei from  $A = 1$  to 208 using Bayesian inference by means of a Hamiltonian Markov Chain Monte Carlo. We used the extracted UMF to correct Deuteron DIS data for structure-modification effects and to extract  $F_2^n/F_2^p$  and hence  $d_v/u_v$  up to  $x_B \approx 0.9$ .

The extracted  $F_2^n/F_2^p$  ratio saturates at high- $x_B$  at a value of  $0.47 \pm 0.04$ . This value is consistent with perturbative QCD and DSE predictions [1, 6], is lower than the SU(6) symmetry prediction of  $2/3$  [42], and is significantly greater than the scalar di-quark model prediction of  $1/4$  [43, 44]. Our Nuclear-DIS analysis prediction also agrees with the most recent experimental extractions by the BonuS experiment [41]. The new BonuS experiment will take data soon and provide a more stringent test of our predictions.

We also used the UMF to predict the Tritium and  $^3\text{He}$  DIS cross section ratios that were recently measured by the MARATHON experiment [45] and to estimate the nuclear correction function  $\mathcal{R}$  that they plan to use to extract  $F_2^n/F_2^p$  from their EMC ratios. We showed that different models of  $\mathcal{R}$  lead to non-negligible model uncertainty in the planned extraction of  $F_2^n/F_2^p$ .

This work was supported by the U.S. Department of Energy, Office of Science, Office of Nuclear Physics under Award Numbers DE-FG02-94ER40818, DE-FG02-96ER-40960, DE-FG02-93ER40771, and DE-AC05-06OR23177 under which Jefferson Science Associates operates the Thomas Jefferson National Accelerator Facility, the Pazy foundation, and the Israeli Science Foundation (Israel) under Grants Nos. 136/12 and 1334/16.

---

\* Contact Author hen@mit.edu

[1] G. R. Farrar and D. R. Jackson, Phys. Rev. Lett. **35**, 1416 (1975).

[2] S. J. Brodsky, M. Burkardt, and I. Schmidt, Nucl. Phys. **B441**, 197 (1995), hep-ph/9401328.

[3] W. Melnitchouk and A. W. Thomas, Phys. Lett. **B377**, 11 (1996), nucl-th/9602038.

[4] R. J. Holt and C. D. Roberts, Rev. Mod. Phys. **82**, 2991 (2010), 1002.4666.

[5] R. D. Ball, E. R. Nocera, and J. Rojo, Eur. Phys. J. **C76**, 383 (2016), 1604.00024.

[6] C. D. Roberts, R. J. Holt, and S. M. Schmidt, Phys. Lett. **B727**, 249 (2013), 1308.1236.

[7] M. Virchaux and A. Milsztajn, Phys. Lett. **B274**, 221 (1992).

[8] L. Frankfurt and M. Strikman, Phys. Rep. **160**, 235 (1988).

[9] M. M. Sargsian et al., J. Phys. **G29**, R1 (2003).

[10] G. A. Miller and J. R. Smith, Phys. Rev. **C65**, 015211 (2002), [Erratum: Phys. Rev. C66,049903(2002)], nucl-th/0107026.

[11] J. R. Smith and G. A. Miller, Phys. Rev. **C65**, 055206 (2002), nucl-th/0202016.

[12] S. Kulagin and R. Petti, Nuclear Physics A **765**, 126 (2006), ISSN 0375-9474.

[13] A. Accardi, L. T. Brady, W. Melnitchouk, J. F. Owens, and N. Sato, Phys. Rev. **D93**, 114017 (2016), 1602.03154.

[14] S. Malace, D. Gaskell, D. W. Higinbotham, and I. Cloet, Int. J. Mod. Phys. **E23**, 1430013 (2014), 1405.1270.

[15] O. Hen, G. A. Miller, E. Piasetzky, and L. B. Weinstein, Rev. Mod. Phys. **89**, 045002 (2017).

[16] S. Dulat, T.-J. Hou, J. Gao, M. Guzzi, J. Huston, P. Nadolsky, J. Pumplin, C. Schmidt, D. Stump, and C. P. Yuan, Phys. Rev. **D93**, 033006 (2016), 1506.07443.

[17] J. Arrington, J. G. Rubin, and W. Melnitchouk, Phys. Rev. Lett. **108**, 252001 (2012), 1110.3362.

[18] A. Tropiano, J. Ethier, W. Melnitchouk, and N. Sato, Phys. Rev. **C99**, 035201 (2019), 1811.07668.

[19] B. Schmookler et al. (CLAS), Nature **566**, 354 (2019).

[20] L. B. Weinstein, E. Piasetzky, D. W. Higinbotham, J. Gomez, O. Hen, and R. Shneor, Phys. Rev. Lett. **106**, 052301 (2011).

[21] O. Hen, E. Piasetzky, and L. B. Weinstein, Phys. Rev. C **85**, 047301 (2012).

[22] O. Hen, D. W. Higinbotham, G. A. Miller, E. Piasetzky, and L. B. Weinstein, Int. J. Mod. Phys. **E22**, 1330017 (2013), 1304.2813.

[23] E. Piasetzky, M. Sargsian, L. Frankfurt, M. Strikman, and J. W. Watson, Phys. Rev. Lett. **97**, 162504 (2006).

[24] R. Subedi et al., Science **320**, 1476 (2008).

[25] I. Korover, N. Muangma, O. Hen, et al., Phys. Rev. Lett. **113**, 022501 (2014).

[26] O. Hen et al. (CLAS Collaboration), Science **346**, 614 (2014).

[27] M. Duer et al. (CLAS), Nature **560**, 617 (2018).

[28] M. Duer et al. (CLAS), Phys. Rev. Lett. **122**, 172502 (2019), 1810.05343.

[29] A. Tang et al., Phys. Rev. Lett. **90**, 042301 (2003).

[30] R. Shneor et al., Phys. Rev. Lett. **99**, 072501 (2007).

[31] E. O. Cohen et al. (CLAS), Phys. Rev. Lett. **121**, 092501 (2018), 1805.01981.

[32] W. Melnitchouk, M. Sargsian, and M. Strikman, Z. Phys. **A359**, 99 (1997).

[33] B. Carpenter, A. Gelman, M. Hoffman, D. Lee, B. Goodrich, M. Betancourt, M. Brubaker, J. Guo, P. Li, and A. Riddell, Journal of Statistical Software, Articles **76**, 1 (2017), ISSN 1548-7660, URL <https://www.jstatsoft.org/v076/i01>.

[34] S. D. Team, *Pystan: the python interface to stan, version 2.17.1.0*, <http://mc-stan.org> (2018).

[35] J. Gomez et al., Phys. Rev. D **49**, 4348 (1994).

[36] J. Seely et al., Phys. Rev. Lett. **103**, 202301 (2009).

[37] N. Fomin et al., Phys. Rev. Lett. **108**, 092502 (2012).

[38] J. Arrington, F. Coester, R. J. Holt, and T. S. H. Lee, J. Phys. **G36**, 025005 (2009), 0805.3116.

[39] J. Arrington, R. Ent, C. Keppel, J. Mammei, and I. Niculescu, Phys. Rev. **C73**, 035205 (2006).

[40] S. A. Kulagin and R. Petti, Phys. Rev. **C82**, 054614 (2010), 1004.3062.

[41] N. Baillie et al. (CLAS), Phys. Rev. Lett. **108**, 142001 (2012), [Erratum: Phys. Rev. Lett. 108, 199902(2012)], 1110.2770.

[42] F. E. Close, *An Introduction to Quarks and Partons* (Academic Press, London, 1979).

[43] F. E. Close, Phys. Lett. **43B**, 422 (1973).

[44] R. D. Carlitz, Phys. Lett. **58B**, 345 (1975).

[45] G. G. Petratos et al., Jefferson Lab PAC37 Proposal (2010), experiment E12-10-103.

[46] V. M. Abazov et al. (D0), Phys. Rev. **D91**, 032007 (2015), [Erratum: Phys. Rev. D91,no.7,079901(2015)], 1412.2862.

[47] L. Whitlow et al., Phys. Lett. **B282**, 475 (1992).

[48] U.-K. Yang and A. Bodek, Phys. Rev. Lett. **82**, 2467 (1999), hep-ph/9809480.

[49] O. Hen, A. Accardi, W. Melnitchouk, and E. Piasetzky, Phys. Rev. D **84**, 117501 (2011).

[50] S. A. Kulagin and R. Petti (private communication).

[51] I. R. Afnan, F. R. P. Bissey, J. Gomez, A. T. Katramatou, S. Liuti, W. Melnitchouk, G. G. Petratos, and A. W. Thomas, Phys. Rev. **C68**, 035201 (2003), nucl-th/0306054.

[52] M. M. Sargsian, S. Simula, and M. I. Strikman, Phys. Rev. **C66**, 024001 (2002), nucl-th/0105052.